Electron-Plasmon and Electron-Electron Interactions at a Single Atom Contact

Guillaume Schull,[1] Nicolas Néel,[1] Peter Johansson,[2] and Richard Berndt[1]

[1]*Institut für Experimentelle und Angewandte Physik, Christian-Albrechts-Universität zu Kiel, D-24098 Kiel, Germany*
[2]*School of Science and Technology, University of Örebro, S-701 82 Örebro, Sweden*

(Received 19 September 2008; revised manuscript received 16 December 2008; published 3 February 2009)

The transition from tunneling to contact is investigated by detecting light emitted from Au(111) in a scanning tunneling microscope. Optical spectra reflect single and multielectron processes and their distinct evolutions as a single-atom contact is formed. The experimental data are analyzed in terms of plasmon excitation and hot-hole processes.

DOI: 10.1103/PhysRevLett.102.057401 PACS numbers: 78.68.+m, 68.37.Ef, 73.20.Mf, 73.63.Rt

Investigations of electron transport through nanoscale contacts involving few or single atoms or molecules have revealed unusual properties which may be relevant for applications in electronic devices. Inelastic effects occurring in such junctions are particularly interesting because they may cause heating, which in turn affects junction stability, but also because they pose challenges for experiments as well as numerical simulations [1]. The excitation of phonons has been observed via spectroscopy of the second derivative of the current-voltage characteristics from point contacts [2] and atomic-scale junctions [3,4]. It was also inferred from enhanced current fluctuations [5] and from irreversible changes of molecules [6] in scanning tunneling microscope (STM) experiments. Inelastic electron-electron scattering, which has been detected in micron-sized metal thin film resistors via shot-noise measurements [7], has been more elusive in atomic-scale contacts. Shot noise from such contacts has been used to investigate the decomposition of conductance values into individual conductance channels [8,9].

Here, electron-plasmon and electron-electron interactions at single-atom contacts are probed via the emission of photons. We present detailed optical spectroscopy of the transition from tunneling to a contact which involves a Au atom adsorbed on a Au(111) single crystal surface as verified by STM imaging. The contacts emit light at photon energies significantly exceeding the applied bias ($h\nu > |eV|$). Model calculations indicate that this emission at elevated currents is due to hot-hole formation and electron-electron interaction at the junction. Simultaneously, one-electron processes are probed by detecting emission at lower photon energies ($h\nu < |eV|$). The one-electron and hot-hole channels display distinctly different characteristics as a contact is formed, giving access to quantum efficiencies of light emission, inelastic electron-plasmon scattering, and two-electron processes at a single-atom contact.

An influence of laser light on the conductance of atomic-size contacts has recently been observed [10]. Various mechanisms—thermal expansion, rectification, plasmon excitation, and photon-assisted transport—were considered, and the latter two were favored by the authors. In the present experiment, mechanisms which involve high photon intensities can be neglected. Spectra of the emitted light directly demonstrate the importance of plasmon excitation. Photon emission at elevated currents from a point contact was attributed to blackbody radiation from a heated electron gas in Ref. [11]. Our results from single adatoms are not consistent with this interpretation.

The experiments were performed with a ultrahigh vacuum STM at low temperature (6.8 K). Au(111) surfaces as well as chemically etched W tips were cleaned by heating and argon ion bombardment. As a final step of the preparation, tips were slightly indented in the sample and, therefore, are most likely Au-coated. These tips exhibit an increased plasmon enhancement compared to pure W tips and also enable reproducible deposition of single Au atoms on the surface. The particularly high tunneling current and voltage bias applied during acquisition of optical spectra can lead to significant modifications of both the tip and the surface. This is why STM topographic images were systematically recorded before and after the acquisition of each spectrum. All data presented here were acquired without changes of the tip or the sample. Photons emitted at the tunneling junction were collected by a lens near the STM and analyzed by a grating spectrometer and liquid nitrogen cooled CCD [12]. Spectra are not corrected for the wavelength-dependent efficiency of the detection equipment, which is displayed as a dashed line in Fig. 1(a).

We first present light emission characteristics from flat Au(111) areas at currents slightly below the transition to contact. In a spectrum of the light emitted at a sample voltage $V = 1.3$ V and a current $I = 5$ μA [Fig. 1(a), solid line], two clear peaks at $h\nu \approx 1.25$ eV and $\approx$1.75 eV are resolved. The high-energy edge of the former peak occurs at $h\nu = 1.3$ eV and obeys the relation $h\nu = eV$ expected for a one-electron process. The light observed at higher $h\nu$ violates this rule, which has successfully been used in modeling light emission by tunneling electrons mediated by localized plasmons [13–15]. Both components of the light emission, which we label "1e" and "2e," respectively, are observed over the wide range of

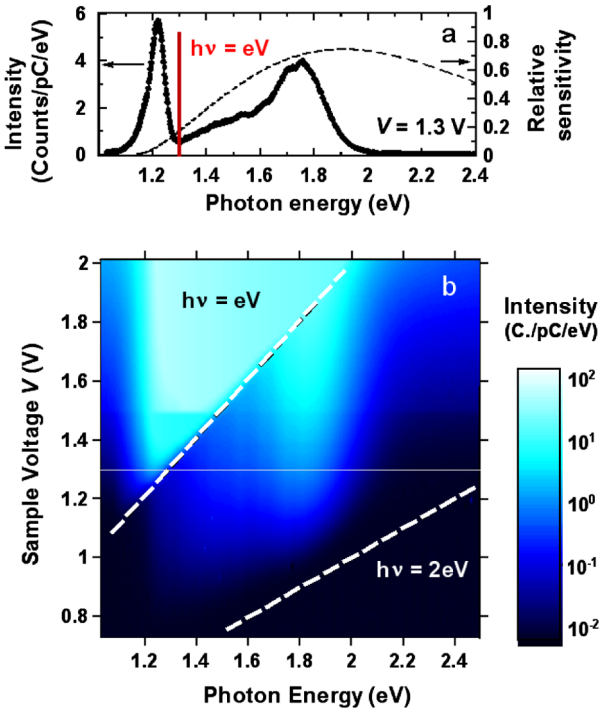

FIG. 1 (color online). (a) Spectrum of the light emitted from a Au-Au junction at $V = 1.3$ V and $I = 5$ μA (solid line) and detector response (dashed line). (b) Series of 64 light emission spectra recorded at V from 0.7 to 2.0 V at 20 mV intervals. Light intensity is represented by false colors on a logarithmic scale. A horizontal line indicates the spectrum shown in (a). To avoid saturation of the CCD camera, spectra have been acquired in two steps below and above 1.46 V with different exposure times. Expected cutoffs for one- ($h\nu < eV$) and two-electron ($eV < h\nu < 2$ eV) processes are indicated by dashed lines.

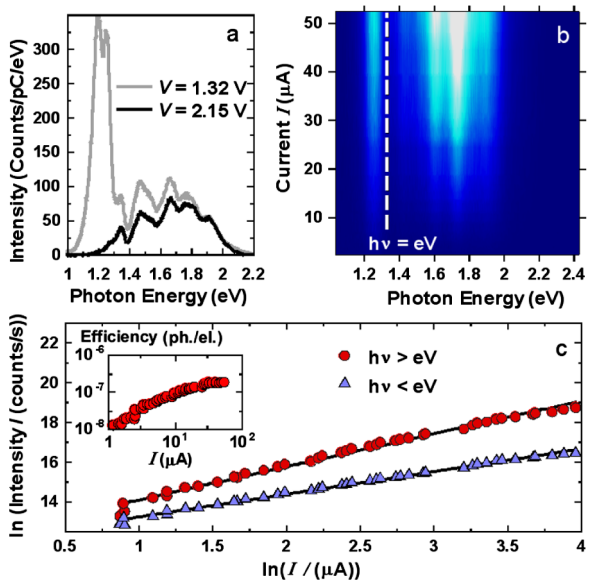

FIG. 2 (color online). (a) Spectra of a Au-Au junction measured—with the same tip and at the same area—at different tunneling conditions: $V = 2.15$ V, $I = 50$ nA (black line); $V = 1.32$ V, $I = 5$ μA (gray line, scaled by a factor of 300). (b) Spectra recorded at 41 tip-sample distances which correspond to 2.4 μA $< I <$ 52.4 μA, with $V = 1.33$ V and an exposure time of 80 ms per spectrum. The logarithm of the light intensity is represented by false color. (c) Total photon intensity vs current I evaluated from (a), for $h\nu < eV$ (triangles) and $h\nu > eV$ (dots). The inset shows the quantum efficiency (photons per electron) of light with $h\nu > eV$.

biases (0.7–2 V) shown in Fig. 1(b). For $V > 2$ V, $1e$ and $2e$ components overlap and cannot be resolved. No photons with $h\nu > 2$ eV are observed. Spectra acquired at reversed bias are similar.

Figure 2(a) shows two spectra recorded at different voltages. The particular tip used gives rise to a rich structure which enables a detailed comparison of the $1e$ and $2e$ components of the emission. At $V = 2.15$ V, $1e$ emission prevails; at 1.32 V, much of the spectrum is due to $2e$ light. Except for low photon energies, both spectra exhibit maxima at identical energies with similar relative intensities. In the case of $1e$ emission, the spectrum is a fingerprint of the plasmons of the nanoresonator, which is comprised of the sample and the specific tip apex [16]. The close similarity of the $2e$ emission is clear evidence that $2e$ light involves the same electromagnetic modes.

Finally, the current dependencies of the emission components were investigated by approaching the tip stepwise to the surface and simultaneously recording fluorescence spectra [Fig. 2(b)]. No major change of the spectral shape of either component was observed with increasing I, implying that the cavity resonances remained largely unchanged over the investigated range of distances in agreement with Ref. [17]. At the particular bias used $V = 1.33$ V, $1e$ and $2e$ emission are quite well separated in the spectra, and their intensities can therefore be evaluated independently by integrating over the respective peaks. The resulting current dependencies [Fig. 2(c)] can be described by power laws $\approx I^{\beta}$. As expected [18], the $1e$ intensity increases almost linearly with I ($\beta \approx 1.1$). For the $2e$ light, $\beta \approx 1.7 \pm 8\%$ was measured repeatedly, indicating that electron-electron interactions are involved in the excitation process. The emission efficiency of the $2e$ light is evolving from $\approx 10^{-8}$ to $\approx 10^{-7}$ photons per electron for the current range displayed in the inset in Fig. 2(c). At a sample voltage of 3 V, a maximum efficiency of $\approx 10^{-4}$ is generally reported for the $1e$ light [13].

Observations of emission with $h\nu > eV$ have previously been reported for Au-Au junctions [11,19] and for Na layers on Cu(111) [20]. In the case of Au-Au junctions, an elevated temperature of the junction was proposed to cause smearing of the Fermi distribution of the electrodes and thus relax the condition $eV > h\nu$ [19]. However, the intensities at photon energies $h\nu - |eV| > 0.6$ eV observed here would require junction temperatures of ≈ 600 K. Such temperatures are not expected according to recent calculations [21]. Moreover, they are difficult

to reconcile with the observed stability of the junctions, which involve a single adatom on flat Au(111) [Fig. 4(a)]. Alternatively, blackbody radiation from a heated electron gas has been invoked [11]. As the shape of our spectra is clearly dictated by plasmon modes and does not match a blackbody spectrum, we discard this interpretation.

The observed $2e$ emission can be explained within the hot-electron-hole cascade mechanism described in Ref. [20] [Fig. 3(a)]. A fraction of the current (arrow 1) is due to elastic tunneling at energies well below the Fermi level E_F of the emitter electrode. A hole deep below E_F can cause a cascade which finally creates hot electrons with energies above E_F (2). Inelastic tunneling of these electrons (3 and 4) couples to localized plasmons of the tip-sample cavity which then leads to $2e$ emission. We have calculated the rate of $2e$-photon emission using a one-dimensional model for the tunnel barrier to determine the energy distribution of the hot holes injected (arrow 1 in Fig. 3). Letting primary and secondary hot holes and electrons diffuse in real space and energy space (see Refs. [22,23] for more details), the energy distribution of hot electrons at the STM tip is calculated. These electrons, through the interaction with localized plasmons in the same way as for $1e$ emission, give rise to light emission with $h\nu > eV$.

Figure 3(b) shows spectra calculated for a bias voltage of 1.2 V and a current of 10 μA. The most striking feature here as well as in the experimental results is that light is emitted with photon energies far above the expected threshold eV. The number of available hot electrons decreases steadily with increasing energy, but the calculated spectra still show a very pronounced peak around 1.7–1.8 eV due to the plasmon modes of the tip-sample system. The calculations predict a quantum efficiency of $\approx 10^{-8}$ photons per electron at $I = 10$ μA and $V = 1.2$ V in reasonable agreement with the experimental value. The intensity of the calculated $2e$-light emission follows a power law $\sim I^{\beta}$, with $\beta \approx 2.1$, thus somewhat above the experimentally observed value. The difference most likely is a result of the difference between the actual 3D potential and the 1D potential used in the calculation.

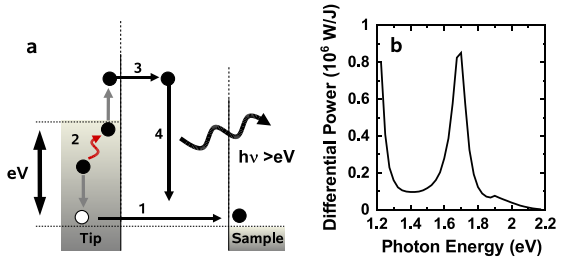

FIG. 3 (color online). (a) Sketch of the hot-hole mechanism leading to the $2e$-light emission. The detailed shape of the barrier, which varies with tip-sample separation, is unknown. (b) Calculated spectra of $2e$ light for $I = 10$ μA and $V = 1.2$ V.

In the case of $2e$-light emission from Na overlayers, an Auger-like mechanism involving electron-electron interaction during tunneling was also considered and found to be similarly important. This mechanism is unlikely to play a significant role here. At close proximity to the tip and the sample, where a point contact is about to be formed, electron-electron interactions within the gap are much more strongly screened than in the Na case with tunneling distances close to 1 nm.

We now focus on the transition to a single-atom contact. Figure 4(a) shows the evolution of the junction conductance as a function of the tip displacement Δz as a Au adatom is approached. Despite the high bias used ($V = 1.35$ V), the conductance trace is similar to low bias data and exhibits a rapid transition from the tunneling range to contact with a conductance $G \approx G_0 = 2e^2/h$. This value of G is typical of a single Au atom between Au electrodes and signals that one perfectly transparent conduction channel is available [24]. Figure 4(b) displays a sequence of emission spectra which were recorded simultaneously with the data in Fig. 4(a). The transition to contact is indicated by an arrow. The overall shape of the spectra remains remarkably constant. However, a distinct difference between $1e$ and $2e$ light is evident. The $1e$ intensity varies smoothly despite the rapid increase of the current as the contact is established. In contrast, the $2e$ intensity in-

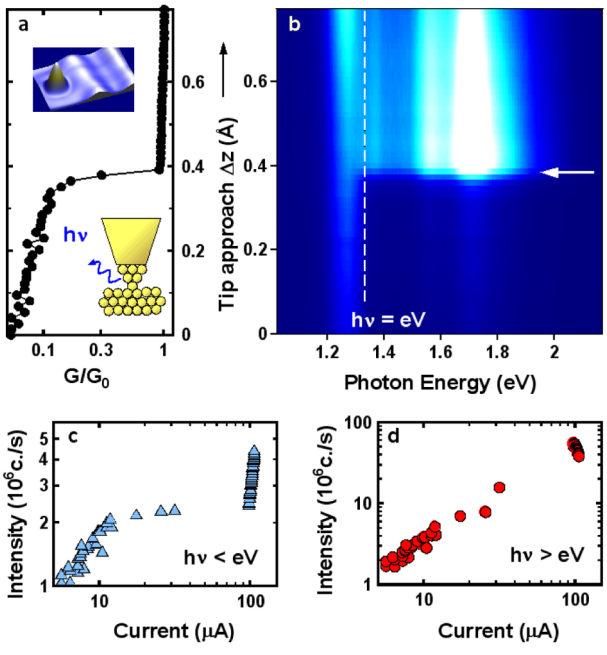

FIG. 4 (color online). (a) Junction conductance in units of G_0 vs tip displacement towards the sample, from tunneling to contact ($V = 1.35$ V). The upper inset shows a STM image of the single adatom remaining on the surface after the contact measurement. (b) Light emission spectra acquired during the tip approach in (a). (c) $1e$- and (d) $2e$-light intensities extracted from (b) by integrating the relevant parts of the spectra.

creases abruptly. Upon further approach of the tip, the $2e$ intensity decreases slowly in $\approx 70\%$ of all experiments although the current continues to increase. Slightly increasing or constant intensities have occasionally been observed, too.

For a more quantitative analysis, Fig. 4(c) shows the integrated intensity of $1e$ light versus I. The behavior observed at nA currents, an approximately linear increase of the intensity with I, prevails up to currents as large as 10 μA. As a contact is formed, additional current (up to 85 μA) flows, but, surprisingly, no increase of the $1e$ intensity is found. Once contact is reached ($I > 95$ μA), a linear increase occurs with a slightly higher slope than in the tunneling range.

The similarity of the spectral shapes indicates that localized plasmon modes, which mediate the $1e$-light emission in the tunneling range, are involved at contact, too. While the contact current may be expected to be largely ballistic, the data reveal that electrons lose energy via plasmon-mediated emission, albeit with a quantum efficiency that is reduced by about a factor of 10, pointing out intriguing variations of the transport properties. We tentatively suggest that the different quantum efficiencies for light emission at contact and in the tunneling range reflect the modified screening of the electrons, which in turn affect the coupling to the electromagnetic field.

The $2e$ light [Fig. 4(d)] provides an additional opportunity to investigate inelastic current contributions. At the transition to contact, the current increases eightfold. In contrast to the constant $1e$ emission, the $2e$ intensity simultaneously grows by a factor of ≈ 6. In repeated measurements, factors varied between 4 and 15. We tentatively interpret this striking difference using the two-step model of Fig. 3(a). $2e$ emission requires a transition well below E_F, which creates a primary hot hole and a subsequent inelastic transition, which excites a photon. As a contact is formed, these two processes are likely to evolve differently. The rate of hot-hole creation is expected to vary approximately linearly with the current. The inelastic decay is virtually identical to the transition involved in $1e$ emission, and its rate thus remains constant. Overall, the $2e$ emission may be expected to grow linearly with I. This is consistent with the data, which reveal an increase of the $2e$ emission upon contact formation, albeit at a lower slope than in the tunneling range. One can estimate the contribution of hot electrons to be $\approx 10^{-4}$ of the total current flowing through a single-atom contact. This can be deduced both from a comparison of the theoretically calculated quantum efficiencies for $1e$ and $2e$ emission ($\approx 10^{-4}$ vs $\approx 10^{-8}$) as well as from the experimental results displayed in Figs. 2(a) and 4.

In summary, the particular sensitivity of optical spectroscopy has been used to probe inelastic contributions to the current flowing through a single atom. By recording the light emitted at a single Au atom contact, the quantum efficiencies of inelastic electron-plasmon scattering and multiple-electron processes have been estimated. They exhibit a distinct change as contact is reached. It seems likely that the experimental approach can be extended to investigate inelastic processes at a variety of atomic and molecular contacts.

We thank Deutsche Forschungsgemeinschaft for financial support.

[1] N. Agrait, A. L. Yeyati, and J. M. van Ruitenbeek, Phys. Rep. **377**, 81 (2003).
[2] A. G. M. Jansen, A. P. van Gelder, and P. Wyder, J. Phys. C **13**, 6073 (1980).
[3] C. Untiedt, G. Rubio Bollinger, S. Vieira, and N. Agraït, Phys. Rev. B **62**, 9962 (2000).
[4] N. Agraït, C. Untiedt, G. Rubio-Bollinger, and S. Vieira, Phys. Rev. Lett. **88**, 216803 (2002).
[5] N. Néel *et al.*, Phys. Rev. Lett. **98**, 065502 (2007).
[6] G. Schulze *et al.*, Phys. Rev. Lett. **100**, 136801 (2008).
[7] A. H. Steinbach, J. M. Martinis, and M. H. Devoret, Phys. Rev. Lett. **76**, 3806 (1996).
[8] H. E. van den Brom and J. M. van Ruitenbeek, Phys. Rev. Lett. **82**, 1526 (1999).
[9] O. Tal, M. Krieger, B. Leerink, and J. M. van Ruitenbeek, Phys. Rev. Lett. **100**, 196804 (2008).
[10] D. C. Guhr *et al.*, Phys. Rev. Lett. **99**, 086801 (2007).
[11] A. Downes, P. Dumas, and M. Welland, Appl. Phys. Lett. **81**, 1252 (2002).
[12] G. Hoffmann, J. Kröger, and R. Berndt, Rev. Sci. Instrum. **73**, 305 (2002).
[13] P. Johansson, R. Monreal, and P. Apell, Phys. Rev. B **42**, 9210 (1990).
[14] Y. Uehara, Y. Kimura, S. Ushioda, and K. Takeuchi, Jpn. J. Appl. Phys. **31**, 2465 (1992).
[15] B. N. J. Persson and A. Baratoff, Phys. Rev. Lett. **68**, 3224 (1992).
[16] J. Aizpurua, S. P. Apell, and R. Berndt, Phys. Rev. B **62**, 2065 (2000).
[17] J. Aizpurua, G. Hoffmann, S. P. Apell, and R. Berndt, Phys. Rev. Lett. **89**, 156803 (2002).
[18] V. Sivel, R. Coratger, F. Ajustron, and J. Beauvillain, Phys. Rev. B **51**, 14 598 (1995).
[19] R. Pechou, R. Coratger, F. Ajustron, and J. Beauvillain, Appl. Phys. Lett. **72**, 671 (1998).
[20] G. Hoffmann, R. Berndt, and P. Johansson, Phys. Rev. Lett. **90**, 046803 (2003).
[21] M. DiVentra, Y.-C. Chen, and M. Zwolak, Nano Lett. **3**, 1691 (2003).
[22] P. Johansson, G. Hoffmann, and R. Berndt, AIP Conf. Proc. **696**, 37 (2003).
[23] R. H. Ritchie, J. Appl. Phys. **37**, 2276 (1966).
[24] M. Brandbyge *et al.*, Phys. Rev. B **52**, 8499 (1995).